

Assessment of Coronary Artery Calcium Using Dual-Energy Subtraction Digital Radiography

John N. Mafi · Baowei Fei · Sharon Roble · Anthony Dota · Prashanth Katrapati · Hiram G. Bezerra · Hesheng Wang · Wei Wang · Leslie Ciancibello · Marco Costa · Daniel I. Simon · Carl E. Orringer · Robert C. Gilkeson

© Society for Imaging Informatics in Medicine 2011

Abstract Cardiovascular disease is the leading cause of global mortality, yet its early detection remains a vexing problem of modern medicine. Although the computed tomography (CT) calcium score predicts cardiovascular risk, relatively high cost (\$250–400) and radiation dose (1–3 mSv) limit its universal utility as a screening tool. Dual-energy digital subtraction radiography (DE; <\$60, 0.07 mSv) enables detection of calcified structures with high sensitivity. In this pilot study, we examined DE radiography's ability to quantify coronary artery calcification (CAC). We identified 25 patients who underwent non-contrast CT and DE chest imaging performed within 12 months using documented CAC as the major inclusion criteria. A DE calcium score was developed based on pixel intensity multiplied by the area of the calcified plaque. DE scores were plotted against CT scores. Subsequently, a validation cohort of 14 additional patients was independently evaluated to confirm the accuracy and precision of CAC quantification, yielding a total of 39 subjects. Among all subjects ($n=39$), the DE score demonstrated a correla-

tion coefficient of 0.87 ($p<0.0001$) when compared with the CT score. For the 13 patients with CT scores of <400, the correlation coefficient was -0.26 . For the 26 patients with CT scores of ≥ 400 , the correlation coefficient yielded 0.86. This pilot study demonstrates the feasibility of DE radiography to identify patients at the highest cardiovascular risk. DE radiography's accuracy at lower scores remains unclear. Further evaluation of DE radiography as an inexpensive and low-radiation imaging tool to diagnose cardiovascular disease appears warranted.

Keywords Calcification detection · Cardiac imaging · Chest CT · Chest radiographs · Computed tomography · Coronary arteries · Coronary calcifications · Coronary disease · Digital radiography · Digital subtraction radiography · Dual-energy subtraction · Radiography · Dual-energy scanned projection · ROC-based analysis

Introduction

Coronary heart disease (CHD) caused one in every six deaths in the USA in 2006 [1]. The current prevention of CHD centers on the identification of risk factors; however, 62.4% of patients with CHD have only zero or one risk factor [2]. The Framingham risk score incompletely assesses risk with a discriminant accuracy of approximately 75% [3].

Computed tomography (CT) has the ability to detect coronary artery calcium (CAC) and has been shown to provide incremental and independent prognostic value to traditional risk factors [4, 5]. CAC has also proven to incrementally add predictive information to the Framingham risk score in diverse racial groups [6]. Although the CT score has shown promise in predicting coronary events,

J. N. Mafi · A. Dota · P. Katrapati · W. Wang
Case Western Reserve University School of Medicine,
2109 Adelbert Rd.,
Cleveland, OH 44106, USA

B. Fei · H. Wang · L. Ciancibello · R. C. Gilkeson (✉)
Department of Radiology,
University Hospitals Case Medical Center,
11100 Euclid Avenue,
Cleveland, OH 44106-5000, USA
e-mail: robert.gilkeson@uhhospitals.org

S. Roble · H. G. Bezerra · M. Costa · D. I. Simon · C. E. Orringer
University Hospitals Harrington-McLaughlin
Heart and Vascular Institute,
11100 Euclid Avenue Lakeside 5038,
Cleveland, OH 44106, USA

its use as a screening tool remains controversial. Two limiting factors include its significant cost (\$250–400) and relatively high ionizing radiation dose (1–3 mSv) [7, 8]. According to recent estimates, screening 50 million individuals with CT scores as proposed by the Screening for Heart Attack and Prevention and Education Taskforce would lead to approximately 6,000 fatal malignancies [9, 10].

Alongside many of the advancements in CT technology, dual-energy subtraction digital radiography (DE) has shown to be promise as a low radiation (0.07 mSv) and inexpensive (<\$60) technique that allows for enhanced visualization of calcified structures over the past 30 years [11–14]. Dual-energy subtraction uses digital processing techniques that both subtract soft tissue structures and optimize visualization of calcified structures, including calcified atherosclerotic plaques. Applying dual-energy subtraction techniques to digital fluoroscopy and real-time video digital radiography, researchers have successfully created methods of CAC quantification [15, 16]. However, these techniques have variable and more extensive radiation doses based on time of exposure. DE radiography's ability to quantify CAC in static chest radiographs of human subjects has not been studied. This pilot study evaluates the feasibility of DE radiography in quantifying CAC compared with the established CT score in human subjects.

Materials and Methods

Study Design

We consecutively identified 25 patients with the following inclusion criteria: all patients who underwent a non-contrasted, non-electrocardiogram (ECG)-gated CT chest study with documented CAC as well as a respective dual-energy subtraction PA digital chest radiograph imaged within 12 months of the CT between 2005 and 2008. These DE scores (details on scoring below) were plotted against their respective CT scores and a receiver operating characteristic (ROC) analysis helped to determine three DE score thresholds that predict a CT score of ≥ 400 : one maximizing positive predictive value (PPV), another maximizing negative predictive value (NPV), and third maximizing both. To confirm the accuracy and precision of CAC quantification and the DE score thresholds, 14 more patients with the same inclusion criteria as above were identified independently as a validation cohort. This study only included patients with positive CAC, and therefore only evaluated DE's ability to quantify, not detect, CAC. Technical exclusion criteria included documented coronary stent, exclusion of part of the heart on the CT scan, and the presence of post-operative metallic staples. The study

protocol of this retrospective analysis was approved by the local institutional review board.

Computed Tomography Protocol

A total of 39 multidetector computed tomography (MDCT) chest studies imaged within 12 months of the respective DE studies were analyzed. The CT exams were non-contrasted, non-ECG-gated, and used 64-slice MDCT (Siemens AG). The CT imaging protocols were fairly standard among all subjects in the study. All CT protocols were reconstructed at 2-mm thickness and 1-mm increment, and at a peak voltage of 120 kV peak (kVp), which is standard at our institution. The reconstruction filters were consistent at b41f, which is also a standard chest soft tissue reconstruction characteristic. The milliamp-seconds (mAs) varied by patient secondary to the use of CT dose modulation techniques. The reference values for mAs ranged between 150 and 180. Finally, the collimation consisted of 16 detectors with 0.75-mm thickness.

CT Calcium Score

An analyst blinded to the DE scores confirmed the presence of CAC and calculated the CT score. The analyst applied the Agatston method [4] to the non-gated CT studies with Siemens AG software. The analyst produced a total score as well as individual scores divided into the four major coronary arterial branches: left main, left anterior descending (LAD), left circumflex, and right coronary artery (RCA).

DE Protocol

Patients were imaged using a direct digital radiography unit (Revolution XRd, GE Healthcare). Using dual-energy digital subtraction, a 60-kVp image is obtained first. Following a 150-ms delay, a conventional 120-kVp image is then performed [18]. Post-processing of the two images produced a conventional 120-kVp image, a subtracted soft tissue image (bone/calcium enhancing or DBone), and a subtracted bone image (soft tissue enhancing or DSoft) [11, 12, 17]. All dual-energy subtraction processing techniques were only performed on the standard posterior–anterior position radiograph, which is identical in orientation and positioning to the conventional posterior–anterior chest X-ray. The lateral image remained only in its conventional format, without dual-energy subtraction processing and was not used in the analysis of this study. Because DE coronary imaging is a new technique, delineating the four major coronary branches on DE radiography has not yet been validated by CT or angiography. Therefore, we compared the total DE score with the total CT score. Based on our

previous work [18, 19], we hope to eventually validate DE coronary imaging with a per-vessel analysis.

DE Coronary Artery Calcium Quantification

The DE score can be defined as the area of the calcified plaque multiplied by the mean pixel intensity of the calcified plaque within the region of interest (ROI). Using Analyze Software System (Copyright Mayo Clinic), a cardiovascular imaging expert blinded to the DE and CT scores independently drew ROIs around the suspected CAC on the DBone (calcium enhancing) images. These ROIs were confirmed by CT axial, coronal, and three-dimensional reconstructions (Figs. 1 and 2). These ROI object maps were then superimposed onto their respective conventional radiograph and the Analyze software calculated the mean pixel intensity as well as the total area of each ROI. Because DE images are two-dimensional, background noise (including myocardium, ribs, and spine) posed limitations in obtaining an accurate pixel intensity of the calcified plaque. Based on previous research [13, 15], we constructed an algorithm to resolve this limitation. By increasing the area of the ROI by 10%, the ROI would cover a thin halo of background noise in addition to the calcified artery. Using the following variables, we designed an equation to subtract background noise by using this thin ring as an extrapolation of the background intensity.

Given,

- N_B Area of ROI (calcified plaque)
- \bar{I}_B Mean pixel intensity of ROI
- N_A Area of scaled ROI (expanded 10% larger)
- \bar{I}_A Mean pixel intensity of scaled ROI

Then,

- $(N_B \times \bar{I}_B)$ T_B or total pixel intensity of ROI (calcified plaque) and
- $(N_A \times \bar{I}_A)$ T_A or total pixel intensity of scaled ROI

Next, we subtract the original ROI from the larger scaled ROI to obtain only background (BG) total pixel intensity:

$$T_A - T_B = T_{BG} \text{ and } T_B - T_{BG} = T_{True}$$

Patients with multiple and distinct calcified lesions had separate ROIs, which were scored separately and summed to yield a final score.

Statistical Analysis

The DE score was divided by 10 [5] to reduce the order of magnitude to that comparable to the typical range of the CT score. The test cohort of 25 was scored and rescored a second time by analyst A to measure intra-observer

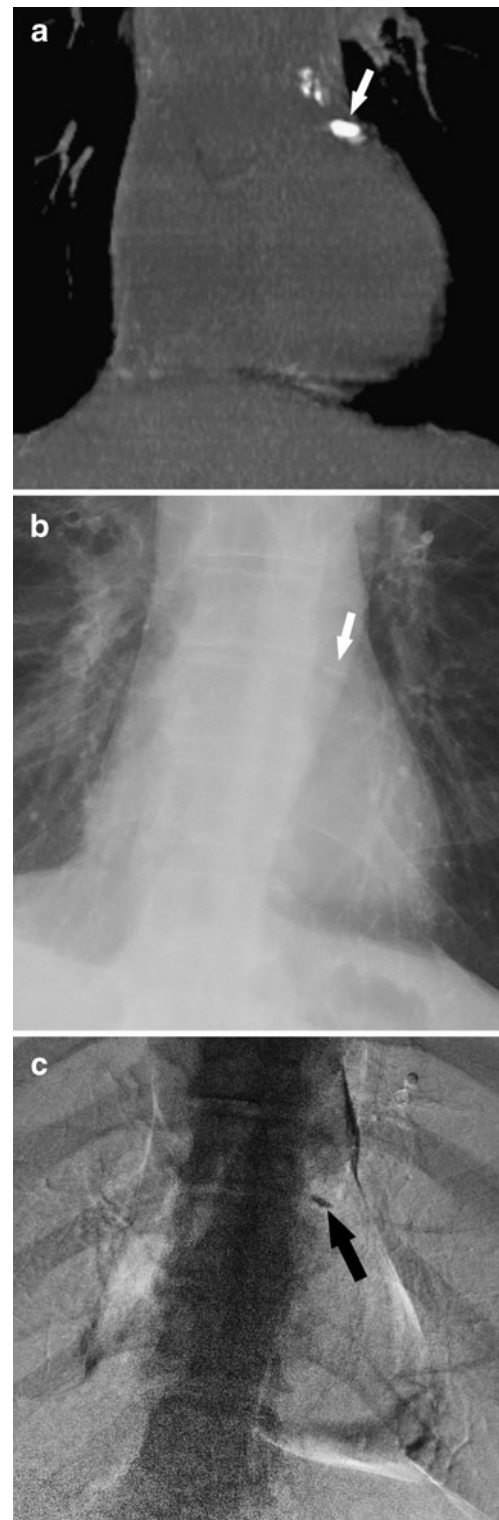


Fig. 1 Detection of CAC by CT and DE: **a** CT coronal reconstruction of CAC in the proximal LAD (*white arrow*). **b** Corresponding standard PA radiograph suspicious for CAC (*white arrow*). **c** Corresponding DE image demonstrating calcification in the region of the LAD (*black arrow*)

variability. To minimize bias from image recall, the second iteration of DE scores were completed 6 months after the

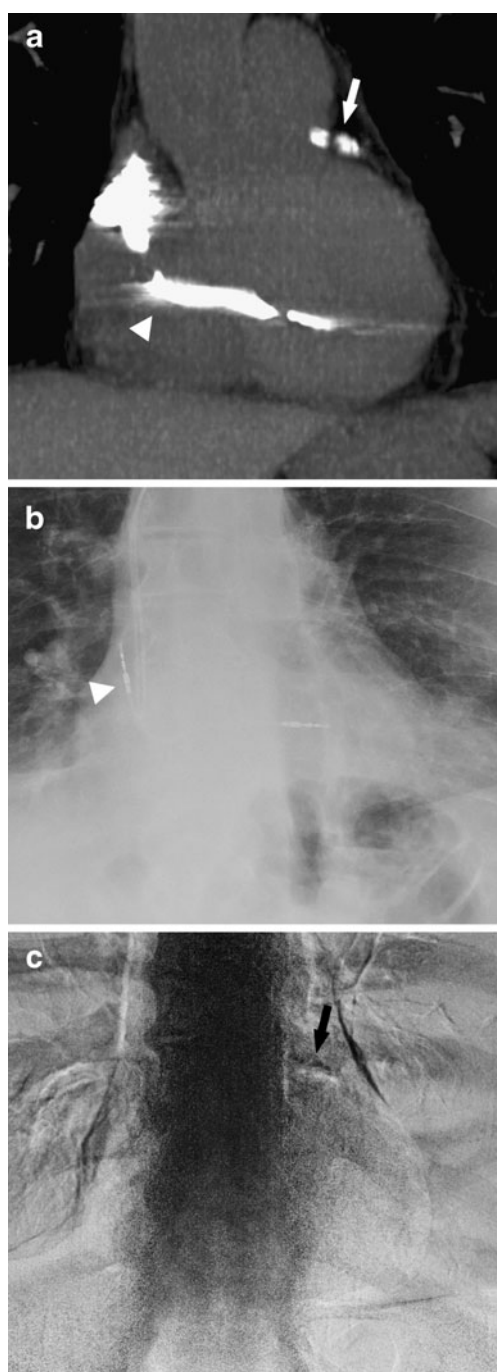


Fig. 2 Detection of CAC by CT and DE: **a** CT coronal reconstruction demonstrating calcium in the LAD, which is marked by the white arrow. The *white arrowhead* points to a pacer wire. **b** Corresponding standard PA radiograph without CAC. The *white arrowhead* points to a pacer wire. **c** Corresponding DE image demonstrating calcification in the region of the LAD

first iteration. The validation cohort of 14 was scored once by analyst A and scored again by a second analyst B to measure inter-observer variability. We also calculated the individual correlation coefficients of the first and second reads among both analysts. The final results comprise an average of the first and second DE score readings.

The statistical analysis was conducted using SAS 9.1 (SAS Institute Inc, Cary, NC, USA), developed by Cytel Software Corporation. PROC CORR was used to obtain the Pearson's correlation coefficients. To test for intra- and inter-observer variability, PROC UNIVARIATE was utilized to calculate the Wilcoxon's signed-rank test and intra-class correlation coefficients (ICC). PROC FREQ with the AGREE option was used to obtain the kappa coefficients. The ROC analysis was obtained by PROC LOGISTICS.

Results

Relevant demographic and clinical characteristics are outlined in Table 1. The average age was 71 years and risk factors such as hypertension, smoking, and CHD were prevalent in this elderly and predominantly Caucasian cohort. The CT scores ranged from 3.3 to 8,899 with a mean of 1,255 and a standard deviation of 1,761. The DE scores ranged from 20 to 1,079, with a mean of 255 and a standard deviation of 248.

Table 1 Characteristics of the study population

| Variable | All subjects ($N=38$) ^a |
|---|--------------------------------------|
| Age (year) | 71±13 |
| Gender (%) | |
| Women | 15 (38) |
| Men | 24 (62) |
| Race (%) | |
| Black | 12 (31) |
| White | 27 (69) |
| History of MI (%) | 6 (16) |
| History of CHD (%) | 15 (40) |
| History of stroke (%) | 7 (18) |
| History of CABG (%) | 11 (29) |
| Hypertension (%) | 31 (82) |
| Dyslipidemia (%) | 25 (66) |
| Plasma cholesterol (mg/dL) ^b | |
| Total | 157±45 |
| LDL | 88±32 |
| HDL | 46±15 |
| Triglycerides | 117±74 |
| Use of lipid-lowering agent (%) | 22 (58) |
| Current or former smoker (%) | 21 (55) |
| Diabetes (%) | 9 (24) |
| Peripheral vascular disease (%) | 2 (5) |
| Chronic kidney disease (%) | 12 (32) |

^a Incomplete data available on 1 of 39 patients (data based on $n=38$)

^b Lipids were obtained on 56% of subjects and only 49% of subjects had complete lipids drawn in this study

Test Cohort

The test cohort of 25 patients yielded a Pearson's correlation coefficient value of 0.89, $p < 0.0001$ (Fig. 3a). Because a CT score of ≥ 400 confers the highest CHD risk (2.4% annual or 24% 10-year risk of myocardial infarction or CHD death) [5], DE thresholds were investigated for the prediction of a CT score of ≥ 400 . An ROC analysis was used to evaluate these thresholds. Because the majority of study subjects had a CT score of ≥ 400 , we chose a threshold that maximized PPV. This threshold corresponded to a DE score of ≥ 270 with a PPV of 100%, NPV of 56%, sensitivity of 56%, and specificity of 100%. In order to confirm the accuracy of CAC quantification, test inter-observer variability of DE scoring, and confirm the validity of the maximal PPV threshold DE score of ≥ 270 , we evaluated a second validation cohort.

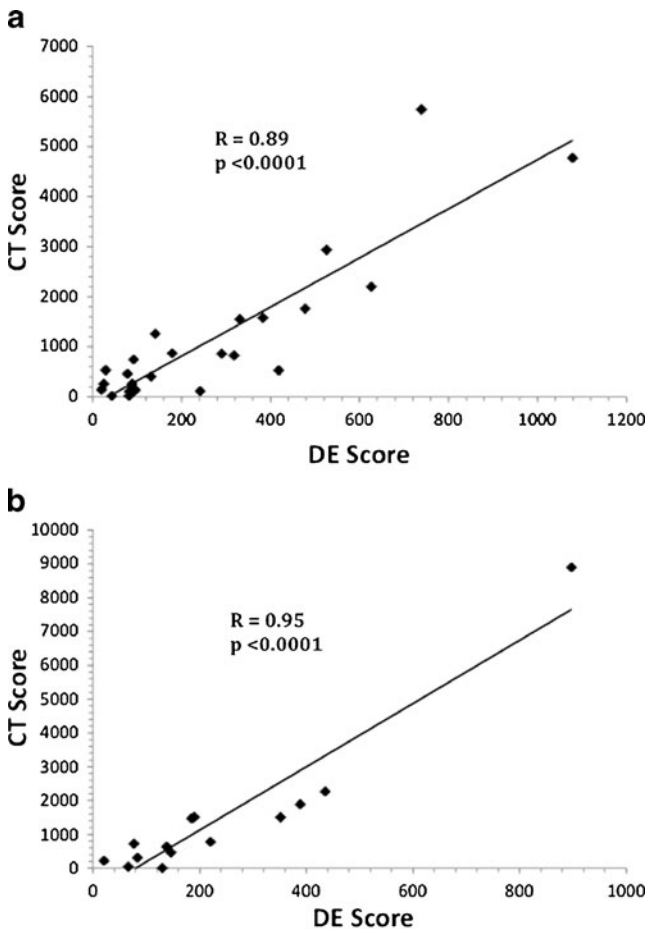


Fig. 3 Correlation of DE and CT scores: **a.** Test cohort DE score versus CT score. The DE scores of the test cohort ($n=25$) are plotted against their respective CT scores. **b.** Validation cohort DE score versus CT score. The DE scores of the validation cohort ($n=14$) are plotted against their respective CT scores

Validation Cohort

The validation cohort of 14 patients yielded a correlation coefficient value of 0.95, $p < 0.0001$ (Fig. 3b). In the validation cohort, analyst A's DE scores confirmed the DE threshold of ≥ 270 with a PPV of 100%, NPV of 40%, sensitivity of 40%, and specificity of 100%. Analyst B's DE scores in the validation cohort also confirmed the DE threshold of ≥ 270 with a PPV of 100%, NPV of 44%, sensitivity of 50%, and specificity of 100%.

Total Cohort

Among all 39 patients in the total cohort, the DE scores demonstrated a positive association with the CT scores with a correlation coefficient value of 0.87, and a p value less than 0.0001. In the total cohort, three different thresholds that corresponded to a CT score of ≥ 400 were investigated. The first threshold optimized positive predictive value or specificity, the second optimized negative predictive value or sensitivity, and the third maximized both positive and negative predictive values (Table 2).

Correlation of DE Scores Versus CT Scores at Low and High Scores

The accuracy of the algorithm at either higher or lower scores was also investigated in the total cohort. For the 13 patients with CT scores of < 400 , the correlation coefficient was -0.26 . For the 26 patients with CT scores of ≥ 400 , the correlation coefficient was 0.86. Stratifying by DE scores yielded the following: for the 25 patients with a DE score of < 270 , the correlation coefficient was 0.51. For the 14 patients with a DE score of ≥ 270 , the correlation coefficient was 0.83.

Intra- and Inter-observer Variability

For the test cohort of 25 subjects, analyst A's first read of DE scores yielded a correlation coefficient of 0.88 when compared with the CT scores. Analyst A's second read yielded $R=0.89$. For the validation cohort of 14 subjects, analyst A's read yielded $R=0.96$ and analyst B's read yielded $R=0.91$.

In the test cohort, a Wilcoxon signed-rank test ($n=25$) between analyst A's first and second scores yielded $p=0.91$, suggesting no significant difference between the two reads. An ICC between analyst A's first and second scores yielded 0.96 demonstrating high agreement. A kappa coefficient measuring agreement with respect to a DE threshold of ≥ 270 predicting a CT score of ≥ 400 yielded 0.92 indicating excellent agreement between analyst A's two sets of scores.

Table 2 Multiple DE thresholds maximizing PPV, NPV, and both

| DE threshold for CT score of ≥ 400 | Sensitivity (%) | Specificity (%) | NPV (%) | PPV (%) |
|---|-----------------|-----------------|---------|---------|
| Maximum PPV (≥ 270) | 54 | 100 | 52 | 100 |
| Maximum NPV (≥ 29) | 100 | 23 | 100 | 72 |
| Maximum PPV and NPV (≥ 130) | 85 | 85 | 73 | 92 |

In the validation cohort, a Wilcoxon's signed-rank test ($n=14$) between analysts A and B again demonstrated no significant difference between the two analysts with a value of $p=0.81$. An ICC analysis between analyst A and B also showed high agreement with a value of 0.96. A kappa coefficient measuring agreement with respect to a DE threshold of ≥ 270 predicting a CT score of ≥ 400 yielded 1.0 indicating excellent agreement between the two analysts.

Discussion

This pilot study demonstrates the feasibility of DE techniques to identify patients at the highest cardiovascular risk. Recent cost-effective analyses have supported the use of CT scores in screening asymptomatic individuals [20]; however, the precise utility of CAC screening awaits a vigorous cost-effective analysis supported by prospective randomized controlled trials [3]. Nonetheless, current American Heart Association and the combined European Society of Cardiac Radiology and North American Society for Cardiovascular Imaging Guidelines have recognized the incremental utility of CAC determination to the Framingham score [5, 21]. Although DE's role in lower scores remains unclear, DE radiography may help to safely and inexpensively risk-stratify patients at high cardiovascular risk. These patients could avoid an unnecessary CT scan, which would reduce the cost and radiation burden associated with CT.

Technical Considerations

The correlation between the DE and CT score is weakest at CT scores of <400 . Possibly, motion artifact and photon scatter are more significant confounders in arteries with smaller calcifications. Nevertheless, the DE score may only crudely estimate low CAC scores, which may only allow for divisions such as low or high plaque burden. Such divisions could still remain clinically useful.

Another potential technical limitation regards the RCA, which may project in front of the spine and impede CAC detection. We calculated that the RCA contributed to 17% of the total calcification quantified on CT. To test whether difficulty visualizing the RCA on DE impedes accuracy, we calculated the correlation using total CT scores that excluded the RCA component. The R value for the total

cohort showed negligible difference (change from 0.87 to 0.86), suggesting that the limited visualization of the RCA on DE imaging was not a significant factor in DE quantification accuracy.

The influence of very high scores on the correlation coefficient was also evaluated. By excluding patients with CT scores of $>2,000$, the correlation coefficient remained reasonably strong at 0.73. Additionally, we assessed the influence of the noise correction algorithm on the DE score's accuracy. When we removed the noise correction algorithm the relationship between the DE and CT scores disappeared, which confirmed the necessity of the correction algorithm. Finally, variations in the noise correction algorithm itself were evaluated. Although the 10% increase in the ROI was arbitrarily chosen as the standard, rates ranging from 5% to 20% increases were also tested, resulting in no significant difference in score accuracy.

Variability in X-ray exposures may also affect the accuracy of the DE score. Technical enhancements such as using a metallic external standard of reference to normalize exposure variabilities (as used in dual-energy X-ray bone absorptiometry) may improve low DE score accuracy [22]. Other strategies such as left-anterior-oblique (LAO) projections to improve RCA visualization and ECG gating and beta blockade to reduce motion artifact may improve the accuracy of lower scores, and such techniques are already under evaluation in our ongoing prospective trial.

DE and the Risk Stratification of CHD

In a recent analysis, researchers found conventional radiography lacking enough sensitivity and specificity to detect CAC [23]. However, computed radiography, DE's predecessor, has been shown to detect the presence of CAC with significantly higher sensitivity than conventional radiography [24]. Our recent pilot study has also demonstrated that DE radiography has better CAC detection capability than conventional radiography [14].

DE radiography's accuracy at high scores might play a complementary role in current CHD screening efforts. However, based on this preliminary data, DE radiography's role as a screening tool remains unclear, particularly for low calcium scores. Choosing a lower threshold DE score of 29 in the ROC analysis allows for 100% sensitivity and a NPV of 100% in predicting CT scores of <400 , which may

contribute to reducing the burden of CT scans. Nevertheless, these preliminary thresholds must be validated by large prospective trials using ECG gating and dual (PA and LAO) projections. If confirmed by future trials, DE could play an integral role in stratifying patients at high risk.

Study Limitations

The DE and CT scores were obtained from non-gated studies. Non-gated images may limit the accuracy and precision of the calculated DE or CT scores. However, according to Wu et al., low-dose ungated multidetector CT showed strong concordance of CT scoring when compared with regular-dose ECG-gated multidetector CT (kappa coefficient=0.89) [25]. Furthermore, a strong correlation coefficient between DE and CT was noted among both cohorts despite the lack of gating. Whether ECG gating would increase the DE score's sensitivity remains to be determined. Moreover, all patients had a positive CT score, which may have affected the overall predictive power of the test, particularly for low DE scores. The impact of including more patients without CAC is difficult to determine at this time, but will be addressed in our ongoing large prospective study. DE radiography's capability in CAC detection has been demonstrated in our previous work [14]. Nonetheless, this paper is an initial pilot study, and rigorous prospective trials are needed before DE radiography can be validated for clinical use.

Conclusions

The results of this pilot study demonstrate the feasibility of DE radiography to identify patients at the highest cardiovascular risk. DE radiography's accuracy at lower scores remains unclear. DE scoring also demonstrates excellent reader agreement without significant intra and inter-observer variability. Further evaluation of DE radiography as an inexpensive and low-radiation imaging tool to diagnose CHD appears warranted.

Acknowledgments We would like to thank Elena DuPont for her assistance in data collection and organization as well as Daniel Prokop for his help in three-dimensional CT reconstructions of the heart. We would also like to thank David Bruckman for his help in statistical analysis. This work was partially supported by NIH grant R21CA120536 (PI: Fei).

References

- Lloyd-Jones D, Adams RJ, Brown TM, et al: Heart disease and stroke statistics—2010 update: a report from the American Heart Association. *Circulation* 121(7):e46–e215, 2010
- Khot UN, Khot MB, Bajzer CT, et al: Prevalence of conventional risk factors in patients with coronary heart disease. *JAMA* 290(7):898–904, 2003
- Weintraub WS, Diamond GA: Predicting cardiovascular events with coronary calcium scoring. *N Engl J Med* 358(13):1394–1396, 2008
- Agatston AS, Janowitz WR, Hildner FJ, et al: Quantification of coronary artery calcium using ultrafast computed tomography. *J Am Coll Cardiol* 15(4):827–832, 1990
- Greenland P, Bonow RO, Brundage BH, et al: ACCF/AHA 2007 clinical expert consensus document on coronary artery calcium scoring by computed tomography in global cardiovascular risk assessment and in evaluation of patients with chest pain: a report of the American College of Cardiology Foundation Clinical Expert Consensus Task Force (ACCF/AHA Writing Committee to Update the 2000 Expert Consensus Document on Electron Beam Computed Tomography) developed in collaboration with the Society of Atherosclerosis Imaging and Prevention and the Society of Cardiovascular Computed Tomography. *J Am Coll Cardiol* 49(3):378–402, 2007
- Detrano R, Guerci AD, Carr JJ, et al: Coronary calcium as a predictor of coronary events in four racial or ethnic groups. *N Engl J Med* 358(13):1336–1345, 2008
- Brenner DJ, Hall EJ: Computed tomography—an increasing source of radiation exposure. *N Engl J Med* 357(22):2277–2284, 2007
- Gerber TC, Carr JJ, Arai AE, et al: Ionizing radiation in cardiac imaging: a science advisory from the American Heart Association committee on cardiac imaging of the council on clinical cardiology and committee on cardiovascular imaging and intervention of the council on cardiovascular radiology and intervention. *Circulation* 119(7):1056–1065, 2009
- Berrington de González A, Mahesh M, Kim K, et al: Projected cancer risks from computed tomographic scans performed in the United States in 2007. *Arch Intern Med* 169(22):2071–2077, 2009
- Stein JH: Radiation and coronary calcium screening. *Am J Cardiol* 100(9):1495, 2007
- Fischbach F, Freund T, Röttgen R, et al: Dual-energy chest radiography with a flat-panel digital detector: revealing calcified chest abnormalities. *AJR Am J Roentgenol* 181(6):1519–1524, 2003
- Brody WR, Butt G, Hall A, Macovski A: A method for selective tissue and bone visualization using dual energy scanned projection radiography. *Med Phys* 8(3):353–357, 1981
- Hickey NM, Niklason LT, Sabbagh E, et al: Dual-energy digital radiographic quantification of calcium in simulated pulmonary nodules. *AJR Am J Roentgenol* 148(1):19–24, 1987
- Gilkeson RC, Novak RD, Sachs P: Digital radiography with dual-energy subtraction: improved evaluation of cardiac calcification. *AJR Am J Roentgenol* 183(5):1233–1238, 2004
- Molloi S, Detrano R, Ersahin A, Roeck W, Morcos C: Quantification of coronary arterial calcium by dual energy digital subtraction fluoroscopy. *Med Phys* 18(2):295–298, 1991
- Xu T, Ducote JL, Wong JT, Molloi S: Feasibility of real time dual-energy imaging based on a flat panel detector for coronary artery calcium quantification. *Med Phys* 33(6):1612–1622, 2006
- Brody WR, Cassel DM, Sommer FG, et al: Dual-energy projection radiography: initial clinical experience. *AJR Am J Roentgenol* 137(2):201–205, 1981
- Chen X, Gilkeson RC, Fei B: Automatic 3D-to-2D registration for CT and dual-energy digital radiography for calcification detection. *Med Phys* 34(12):4934–4943, 2007
- Fei B, Chen X, Wang H, et al: Automatic registration of CT volumes and dual-energy digital radiography for detection of cardiac and lung diseases. *Conf Proc IEEE Eng Med Biol Soc* 1:1976–1979, 2006
- Shaw LJ, Raggi P, Berman DS, Callister TQ: Cost effectiveness of screening for cardiovascular disease with measures of coronary calcium. *Prog Cardiovasc Dis* 46(2):171–184, 2003

21. Oudkerk M, Stillman AE, Halliburton SS, et al: Coronary artery calcium screening: current status and recommendations from the European Society of Cardiac Radiology and North American Society for Cardiovascular Imaging. *Int J Cardiovasc Imaging* 24 (6):645–671, 2008
22. Lukaski HC: Soft tissue composition and bone mineral status: evaluation by dual-energy X-ray absorptiometry. *J Nutr* 123(2 Suppl):438–443, 1993
23. Mahnken AH, Wein BB, Sinha AM, Günther RW, Wildberger JE: Value of conventional chest radiography for the detection of coronary calcifications: comparison with MSCT. *Eur J Radiol* 69 (3):510–516, 2009
24. Sakuma H, Takeda K, Hirano T, et al: Plain chest radiograph with computed radiography: improved sensitivity for the detection of coronary artery calcification. *AJR Am J Roentgenol* 151(1):27–30, 1988
25. Wu M, Yang P, Huang Y, et al: Coronary arterial calcification on low-dose ungated MDCT for lung cancer screening: concordance study with dedicated cardiac CT. *AJR Am J Roentgenol* 190 (4):923–928, 2008

Mafi J, Fei B, Roble S, Dota A, Katrapati P, Bezerra HG, Wang H, Wang W, Ciancibello L, Costa M, Simon DI, Orringer CE, Gilkeson RC. Assessment of coronary artery calcium using dual-energy subtraction digital radiography. *Journal of Digital Imaging* (2011)

Copyright 2011 Springer. One print or electronic copy may be made for personal use only. Systematic reproduction and distribution, duplication of any material in this paper for a fee or for commercial purposes, or modification of the content of the paper are prohibited.

[http:// DOI 10.1007/s10278-011-9385-y](http://doi.org/10.1007/s10278-011-9385-y)